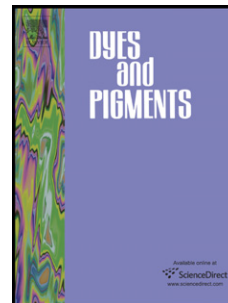


Accepted Manuscript

Synthesis, third-order nonlinear optical properties and theoretical analysis of vinylferrocene derivatives

Jianhong Jia, Yanhong Cui, Yujin Li, Weijian Sheng, Liang Han, Jianrong Gao



PII: S0143-7208(13)00060-0

DOI: [10.1016/j.dyepig.2013.01.028](https://doi.org/10.1016/j.dyepig.2013.01.028)

Reference: DYPI 3857

To appear in: *Dyes and Pigments*

Received Date: 6 December 2012

Revised Date: 28 January 2013

Accepted Date: 31 January 2013

Please cite this article as: Jia J, Cui Y, Li Y, Sheng W, Han L, Gao J, Synthesis, third-order nonlinear optical properties and theoretical analysis of vinylferrocene derivatives, *Dyes and Pigments* (2013), doi: 10.1016/j.dyepig.2013.01.028.

This is a PDF file of an unedited manuscript that has been accepted for publication. As a service to our customers we are providing this early version of the manuscript. The manuscript will undergo copyediting, typesetting, and review of the resulting proof before it is published in its final form. Please note that during the production process errors may be discovered which could affect the content, and all legal disclaimers that apply to the journal pertain.

Highlights

A series of vinylferrocene derivatives were synthesized

The third-order nonlinear optical properties were measured using femtosecond degenerate four-wave mixing.

The energy of the Highest Occupied Molecular Orbital (HOMO), the Lowest Unoccupied Molecular Orbital (LUMO), the energy gap of the HOMO and LUMO (E_{gap}), natural charge, and molecular orbitals are performed by the Density Function Theory (DFT)

ACCEPTED MANUSCRIPT

Synthesis, third-order nonlinear optical properties and theoretical analysis of vinylferrocene derivatives

Jianhong Jia, Yanhong Cui, Yujin Li, Weijian Sheng, Liang Han and Jianrong Gao*

State Key Laboratory Breeding Base of Green Chemistry-Synthesis Technology, Zhejiang University of Technology, Hangzhou

310014, P R China

Abstract: A series of vinylferrocene derivatives were synthesized from the reaction of ferrocenecarboxaldehyde, alcohol, and triphenylphosphonium bromide in a one-pot, solid-state reaction. Their third-order nonlinear optical (NLO) properties were evaluated in N,N-dimethylformamide at 800 nm using femtosecond degenerate four-wave mixing. The third-order NLO susceptibilities of the compounds were $2.55\sim 3.78\times 10^{-13}$ esu. The second-order hyperpolarizabilities of the molecules were $2.42\sim 3.60\times 10^{-31}$ esu. The response times were 51~98 fs. The energy of the Highest Occupied Molecular Orbital (HOMO), the Lowest Unoccupied Molecular Orbital (LUMO), the energy gap of the HOMO and LUMO (E_{gap}), natural charge, and molecular orbitals are performed by the Density Function Theory (DFT). The DFT study showed that the third-order NLO properties were increased with the increasing electron-withdrawing ability in accordance with the decreasing E_{gap} and the increasing charge transfer among the donor, π -bridge, and the acceptor. The experiment and theoretical results show that the vinylferrocene derivatives have potential nonlinear optical applications.

Keywords: vinylferrocene derivatives; nonlinear optics; DFWM technique; the third-order NLO; functional dyes; density function theory

1. Introduction

Third-order NLO materials had received wide attention in material science due to their possible applications in the fabrication of devices related to telecommunications, optical computing, optical storage, and optical information processing[1-6]. Organic materials had been investigated as alternatives to inorganic species due to their low cost, fast and large nonlinear response over a broad frequency range, inherent synthetic flexibility, high optical-damage threshold, and intrinsic tailorability[7-10]. The basic structure of NLO materials are based on the π -bond system. The delocalization of an electronic charge distribution arising from π -orbital overlap leads to a high mobility of the electron density. Many studies had focused on the structure-property trends of donor-acceptor strengths and the effectiveness of different conjugated backbones[11-18]. Incorporation of a metal atom as the center of the macrocycle results in two types of charge-transfer transitions, namely, metal-to-ligand and ligand-to-metal. The molecular hyperpolarizability may be enhanced by metal-ligand bonding through the transfer of the electron density between the metal atom and the conjugated ligand systems. The vinylferrocene moiety has been used as a π -electron donor in several compounds because of its highly conjugated two-dimensional π -electron system, which produces a large nonlinear optical response[19-27].

In the present work, a new convenient approach for the high-yield synthesis of vinylferrocene derivatives from the reaction of ferrocenecarboxaldehyde, alcohol, and triphenylphosphonium bromide in a one-pot, solid-state reaction without the use of

phosphorus ylides is described (Fig. 1). The third-order NLO properties were measured using the femtosecond time-resolved degenerate four-wave mixing (DFWM) technique. And the quantum chemistry study was performed on six compounds with the DFT. The excellent NLO properties were illustrated from the energy of the HOMO, the LOMO, energy gap of the E_{gap} , natural charge, and MOs. This is the first study of the NLO properties for these compounds both in experiment and quantum chemistry.

Fig. 1

2 Experimental section

2.1 Materials

Unless otherwise stated, starting materials were used as purchased without further purification. The dimethylformamide (DMF) was distilled from CaH_2 .

2.2 Instruments

Infrared spectra were recorded on a Vector 22 FT-IR spectrometer using KBr pellets. The ^1H nuclear magnetic-resonance (^1H MNR) spectra were obtained on a Varian XL-200 spectrometer. Ultraviolet-visible (UV-vis) spectra were recorded on a Shimadzu UV-2550 UV-visible spectrophotometer using a quartz cuvette with a 1 cm path length. Elemental analyses were performed on a Carlo ERBA 1106 elemental analyzer. The two reaction vessels were milled simultaneously in a Retsch MM301 mixer mill (Retsch GmbH, Haan, Germany) at a frequency of 30 Hz for 0.5 h.

2.3 Synthesis

2.3.1 Ferrocenecarboxaldehyde (1)

A mixture of 5.3 g (28 mmol) ferrocene and 60 mL chloroform was placed in a 50 mL three-neck flask and kept at -5 to -10°C. Afterward, 10.5 mL phosphorus oxychloride dissolved in 15 mL DMF was added for 1.5 h. The resulting reaction mixture was refluxed for 12 h. After solvent removal, the product was poured into 100 mL ice water and filtered. The filtrate was neutralized to pH 8-9 using NaOH (10%, w/v) and then extracted with ether. The organic layer was washed with water and dried over anhydrous MgSO₄. After removal of the solvent, the crimson solid was recrystallized from n-hexane. The purified product (1) weighed 2.3 g (79% yield). ¹H NMR(CDCl₃): δ, 9.95 (s, 1H, HC=O), 4.79-4.80 (d, 2H, Cp-rings), 4.60-4.61(d, 2H, Cp-rings), 4.28(s, 5H, Cp'-rings). MS(ESI), m/z: 215.0 (M+) FT-IR (KBr): ν(cm⁻¹) 1681(C=O).

2.3.2 Ferrocenyl-2-phenylethylene (2a)

A mixture of 0.214 g (1 mmol) ferrocenecarboxaldehyde, 0.108 g (1 mmol) benzalcohol, 0.343 g (1 mmol) triphenylphosphonium bromide, and 0.04 g (1 mmol) NaOH was ball milled at room temperature for 0.5 h. The procedure was monitored by thin-layer chromatography. The mixture was extracted in 20 mL dichloromethane. After filtration, the solvent was removed under vacuum to obtain the crude product. The residue was chromatographed on silica gel using petroleum ether with CH₂Cl₂ (1:1) as the eluent. The product is a red powder with a yield of 75.2%, as identified using ¹H NMR (500 MHz, CDCl₃): δ 7.45 (d, J=7.5 Hz, 4H, Ar-H), 7.35 (d, J=7.5 Hz,

4H, Ar-H), 7.31 (dd, J=14.3, 6.9 Hz, 4H), 7.24 (t, J=6.7 Hz, 3H), 6.89 (dd, J=16.1 Hz, 2H, CH=CH), 6.72 (d, J=16.2 Hz, 2H, CH=CH), 6.45 (d, J=12.0 Hz, 1H, CH=CH), 6.33 (d, J=11.9 Hz, 1H, CH=CH), 4.48 (s, 4H, C₅H₄), 4.35-4.21 (s, 4H, C₅H₄), 4.21-4.14 (m, 14H, C₅H₄/C₅H₅), 4.11 (d, J=3.3 Hz, 5H, C₅H₅). MS (ESI), m/z: 288.1 (M⁺). FT-IR (KBr), ν (cm⁻¹): 2920(=C-H), 1600 (-C=C-), 960, 753; UV-Vis (CH₂Cl₂) λ (nm): 263.5, 280.0, 310.0. From this experiment, the other yields are as follows:

2.3.3 Ferrocenyl-2-(4-methoxyphenyl)ethylene (2b)

Red powder; yield 63.0%. ¹H NMR (500 MHz, CDCl₃) δ 7.40 – 7.36 (m, 8H, Ar-H), 7.29 (s, 2H, Ar-H), 6.93-6.85 (m, 8H, Ar-H), 6.85-6.81 (m, 2H, Ar-H), 6.72 (dd, 4H, CH=CH), 6.68 (dd, 4H, CH=CH), 6.37 (dd, 1H, CH=CH), 6.27 (dd, 1H, CH=CH), 4.45 (t, J=1.8 Hz, 8H, C₅H₄), 4.30-4.24 (m, 8H, C₅H₄), 4.19 (t, J=1.8 Hz, 2H, C₅H₄), 4.16 (d, J=1.9 Hz, 2H, C₅H₄), 4.14 (s, 20H, C₅H₅), 4.11 (s, 5H, C₅H₅), 3.84 (s, 12H, OCH₃), 3.83 (s, 3H, OCH₃). MS (ESI), m/z: 318.0 (M⁺). FT-IR (KBr), ν (cm⁻¹): 3091 (C-H), 1636 (-C=C-) λ (nm): 290.0.

2.3.4 Ferrocenyl-2-(3-nitro-phenyl)ethylene (2c)

Red powder; yield 81.4%. ¹H NMR (500 MHz, CDCl₃) δ 8.30 (t, J=1.9 Hz, 2H, Ar-H), 8.24 (s, 1H, Ar-H), 8.13 – 8.01 (m, 3H, Ar-H), 7.71 (d, J=7.8 Hz, 2H, Ar-H), 7.67 (d, J=7.7 Hz, 1H, Ar-H), 7.49 (t, J=8.0 Hz, 2H, Ar-H), 7.44 (t, J=8.0 Hz, 1H, Ar-H), 7.05 (dd, J=16.1 Hz, 2H, CH=CH), 6.74 (dd, J=16.1 Hz, 2H, CH=CH), 6.50 (dd, J=11.9 Hz, 1H, CH=CH), 6.43 (dd, J=11.9 Hz, 1H, CH=CH), 4.52 (s, 4H, C₅H₄), 4.39-4.34 (s, 4H, C₅H₄), 4.24 (d, J=20.0, 18.2 Hz, 4H, C₅H₄), 4.18 (d, J=2.8 Hz, 10H,

C_5H_5), 4.15 (s, 5H, C_5H_4). MS (ESI), m/z: 333.0 (M⁺). FT-IR (KBr), ν (cm^{-1}): 3091 (C-H), 1633(-C=C-). λ (nm): 290.0.

2.3.5 Ferrocenyl-2-(2,4-dichloro-phenyl)ethylene (2d)

Red powder; yield 74.3 %. 1H NMR (500 MHz, $CDCl_3$) δ 7.56 (d, J=8.5 Hz, 3H, Ar-H), 7.46 (t, J=3.3 Hz, 2H, Ar-H), 7.40 (d, J=2.1 Hz, 3H, Ar-H), 7.31 (d, J=13.2, 6.4 Hz, 2H, Ar-H), 7.23 (d, J=8.5, 2.1 Hz, 3H, Ar-H), 7.16 (d, J=2.0 Hz, 2H, Ar-H), 7.01 (dd, 3H, CH=CH), 6.89 (dd, 3H, CH=CH), 6.46 (dd, J=11.8 Hz, 2H, CH=CH), 6.37 (dd, J=11.8 Hz, 2H, CH=CH), 4.52 (t, J=1.7 Hz, 6H, C_5H_4), 4.35 (t, J=1.7 Hz, 6H, C_5H_4), 4.18 (s, 19H, C_5H_4 , C_5H_5), 4.07 (s, 19H, C_5H_4 , C_5H_5). MS (ESI), m/z: 356.0 (M⁺). FT-IR (KBr), ν (cm^{-1}): 3093 (C-H), 1625(-C=C-) λ (nm): 280.0, 328.5.

2.3.6 Ferrocenyl-2-furanoethylene (2e)

Red powder; yield 85.5%. 1H NMR (500 MHz, $CDCl_3$) δ 7.35 (d, J=5.9 Hz, 12H, C_4H_3O), 6.77 (d, J=16.1 Hz, 6H, CH=CH), 6.49 (dd, J=16.1 Hz, 6H, CH=CH), 6.37 (m, J=10.2, 3.9 Hz, 24H, C_4H_3O), 6.19 (d, J=3.2 Hz, 6H, C_4H_3O), 6.15 (s, 16H, CH=CH), 4.55 (s, 16H, C_5H_4), 4.40 (s, 12H, C_5H_4), 4.25 (d, J=1.7 Hz, 28H, C_5H_4), 4.11 (d, J=4.7 Hz, 70H, C_5H_5). MS (ESI), m/z: 279.1 (M⁺). FT-IR (KBr), ν (cm^{-1}): 3095 (C-H), 1636(-C=C-). λ (nm):295.5.

2.3.7 Ferrocenyl-2-thiophenethylene (2f)

Red powder; yield 70.1%. 1H NMR (500 MHz, $CDCl_3$) δ 7.14 (d, J=13.9 Hz, 2H, C_4H_3S), 7.04 (s, 1H, C_4H_3S), 6.95 (d, J=8.4 Hz, 3H, C_4H_3S), 6.82 (dd, J=15.9 Hz, 1H, CH=CH), 6.68 (dd, J=15.6 Hz, 1H, CH=CH), 6.47 (dd, J=12.1 Hz, 1H, CH=CH), 6.31 (dd, J=11.7 Hz, 1H, CH=CH), 4.42 (s, 2H), 4.37 (s, 2H, C_5H_4), 4.27 (s, 2H,

C₅H₄), 4.23 (s, 2H, C₅H₄), 4.11 (d, J=25.1 Hz, 10H, C₅H₅). MS (ESI), m/z: 294.0 (M⁺). FT-IR (KBr), ν (cm⁻¹): 3101 (C-H), 1626(-C=C-) λ (nm): 278.5, 314.2.

2.4 Nonlinear optical measurements

The third-order NLO properties were measured by the femtosecond DFWM technique using a Ti: sapphire laser. The pulse width was 80 fs, as measured on an SSA25 autocorrelator. The operating wavelength was centered at 800 nm. The repetition rate of the pulses was 1 kHz. During the measurement, the laser was very stable (rms < 0.1%). The input beam was split into two beams (k1 and k2) of nearly equal energies using a beam splitter, which were focused on the sample plot. The k2 beam passed through a delay line driven by a stepping motor so that the optical path length difference between the k2 and k1 beams could be adjusted during the measurement. The angle between the beams was about 5°. When the beams were overlapped spatially in the sample, the generated signal beam passed through an aperture, which was recorded by a photodiode, and then analyzed by a lock-in amplifier and computer (Fig. 2).

The experiments were performed at 22 °C in DMF solutions using a 1 mm-thick quartz cell. As a reference, the optical nonlinearity of the standard sample (CS₂) was also observed.

Fig. 2

2.5 Calculated method

The ground-state geometry optimizations of all isomers were performed by using DFT method with B3LYP[28]. The basis set used was 6-31G (d). The vibrational

frequencies were calculated with the same basis set. All the predicated vibrational spectra had no imaginary frequency, which implied that the optimized geometries were locating at the local lowest point on the potential energy surface[29]_ENREF 27 ENREF 27. Upon the optimized structures predicted by B3LYP/6-31g (d) level, the MOs and natural charge analyses at the same level of theory were carried out for isomers. Time-dependent-DFT calculations of the single excitation energies were performed at the optimized geometries of the ground states, and the basis set used was 6-31G (d). All the calculations were performed within the Gaussian 09 quantum chemical package[30]_ENREF 28 ENREF 27.

3. Results and discussion

Among the six vinylferrocene derivatives, 2d is a new compound[31-34]. The compounds were synthesized by the Vilsmeier reaction and the solid-state Wittig reaction, as illustrated in Fig. 1.

The linear UV-vis absorption spectra of the six vinylferrocene derivatives in DMF solutions are shown in Fig. 3. These compounds exhibited absorption peaks between 260 and 330 nm. The laser wavelength (800 nm) used in the DFWM experiment was far from their resonant bands. Thus, the third-order NLO susceptibilities $\chi^{(3)}$ of the compounds were off-resonant nonlinear responses.

Fig. 3

The third-order NLO susceptibility, $\chi^{(3)}$, is calculated by comparing the measured signal for the sample with that for CS₂ under the same experimental condition. The $\chi^{(3)}$ is obtained according to the following formula[35]_ENREF 27:

$$\chi_s^{(3)} = \left(\frac{I_s}{I_r} \right)^{1/2} \frac{L_r}{L_s} \left(\frac{n_s}{n_r} \right)^2 \frac{\alpha L \exp(\alpha L / 2)}{1 - \exp(-\alpha L)} \chi_r^{(3)} \quad (1)$$

Where I is the intensity of the phase-conjugated beam, L is the sample path length, n is the linear refractive index, and α is the linear absorption coefficient. The subscripts 's' and 'r' refer to the sample and CS₂, respectively. The fraction $\frac{\alpha L \exp(\alpha L / 2)}{1 - \exp(-\alpha L)}$ comes from the sample absorption and equals to 1 approximately while the sample has little absorption around the employed laser wavelength (800 nm). The fraction $\frac{L_r}{L_s}$ equals to 1 approximately while the sample and CS₂ were detected with the same pool in our experiment. Thus, the equation (1) might be modified as follows:

$$\chi_s^{(3)} = \left(\frac{I_s}{I_r} \right)^{1/2} \left(\frac{n_s}{n_r} \right)^2 \chi_r^{(3)} \quad (2)$$

The values of $\chi_r^{(3)}$ and n_r for CS₂ are 6.7×10^{-14} esu and 1.632, respectively[36-38].

The values of n_s for the sample were measured by 2WAJ Abbe refractometer.

The second hyperpolarizability γ of a molecule in isotropic media is related to the solution $\chi^{(3)}$ by:

$$\gamma = \frac{\chi^{(3)}}{Nf^4} \quad (3)$$

Where f^4 is the local field correction factor which is $[(n^2 + 2)/3]^4$ (n is the linear refractive index of the solution), $N = N_A \cdot C/M$ is number of solution molecules per unit volume and N_A is Avogadro number.

The nonlinear refractive index n_2 in isotropic media is estimated through the follow equation (4).

$$n_2 = \frac{12\pi\chi^{(3)}}{n_r^2} \quad (4)$$

The temporal response of the phase conjugate signal as a function of the delay time of the input beam is shown in Fig. 4. The response times (τ) of the samples is half-peak width, and the intensity of the optical conjugate wave (I) is peak height.

The values of $\chi^{(3)}$, n_2 , γ and response times for the samples deduced and calculated from the experimental results are listed in Table 1.

Fig. 4

Table 1.

The vinylferrocene derivatives 2a–2f possess a highly delocalized π -conjugated electron system. The γ values of the vinylferrocene derivatives are higher than that of the other third-order NLO materials, such as organobimetallic Ru(II)-Re(I) 4-ethynylpyridyl complexes[39]_ENREF_30, which is about 6×10^{-34} esu, and are also higher than that of ferrocene, which is 1.6×10^{-35} esu[40]_ENREF_30.

The fully optimized geometries of the six compounds were shown in Fig. 5. All the C atoms of one cyclopentadiene in ferrocene, the ethylene, and the benzene ring are almost in the one plane with the 1.4° largest dihedral angle. This excellent coplanarity implies these compounds could have good third order NLO property. The energy of HOMO, LUMO, and the E_{gap} were listed in Table 2. The electron-withdrawing substituents aryl (e.g. $-\text{NO}_2$ and $-\text{2Cl}$) decrease the energy of LUMO and HOMO-LUMO E_{gap} as shown in Fig. 6. The lower energy of LUMO illustrates the electron injection was improved. The lower E_{gap} illustrates these compounds with

electron-withdrawing substituents aryl would have larger three-order NLO which accord with the above experiment as well.

Table 2.

Fig. 5

Fig. 6

These derivatives contain electron-withdrawing substituents aryl radical groups and electron-donating ferrocenyl in the form of a D- π -A structure, resulting in a stronger intermolecular charge transfer. Then the natural charges of 2a to 2d were calculated listed in Table 3. Electron-withdrawing substituents such as the -NO₂ and -2Cl have higher natural charge values (-0.07 e) than that of 2a (-0.03 e) and 2b (-0.01 e). The natural charge of the -CH=CH- bridge is increased with the increasing of the electron-withdrawing ability of the substituents such as the -Cl has 0.06 larger than that of -OCH₃. The charge transfer among the D, -CH=CH- bridge, and the substituents are accord with the γ values of these complexes. The stronger is the electron-withdrawing ability of the substituents of the aryl groups, the higher are the γ values.

Table 3.

On the basis of the optimized ground geometry, the significant excited states are calculated with TD-DFT. For the majority of the excited states with the largest oscillator strengths, the electron translates mainly from the HOMO-2 to LUMO when the substituents are not -NO₂ (mainly from the HOMO-2 to LUMO+1). In order to

illustrate the differences, the frontier molecular orbitals (FMOs) of 2a to 2f compounds are listed in Fig. 7. The FMOs (LUMO+2, LUMO+1, LUMO, HOMO, HOMO-1, and HOMO-2) of the six calculated isomers are similar to each other in principal character except the substituents of $-\text{NO}_2$. The reverse of the LUMO and LUMO+1 in the complex with the substituents on benzene ring is $-\text{NO}_2$ results the more difficult transition of electron from HOMO-2 to LUMO+1. Therefore, the complex with $-\text{NO}_2$ has smaller coefficient of third-order NLO than the complex with two $-\text{Cl}$. The HOMO-2 is mainly composed by the p atomic orbital of C in cyclopentadiene, $-\text{CH}=\text{CH}-$, and $-\text{Ph}$. The HOMO-1 mainly located on the ferrocene, especially the d atomic orbital of Fe atom. The HOMO is mainly contributed by the p atomic orbital of C in cyclopentadiene and $-\text{CH}=\text{CH}-$. The π^* is formed between the cyclopentadiene and $-\text{CH}=\text{CH}-$ in HOMO-2, and HOMO. However, the cyclopentadiene and $-\text{CH}=\text{CH}-$ formed π bond with p atomic orbital of C.

Fig. 7

4. Conclusions

Six vinylferrocene derivatives possessing D- π -A structures were synthesized by a one-pot solid-state reaction, and characterized by UV, IR, and ^1H NMR spectroscopy. The third-order NLO properties in the femtosecond range were investigated using the DFWM technique at 800 nm. The γ values increase with the strength of electron-accepting characteristics. The γ value of heterocyclic radical groups is higher than that of aryl groups. These compounds possess ultrafast response times of < 98 fs. The DFT study showed that the third-order NLO properties were increased with the

increasing electron-withdrawing ability in accordance with the decreasing E_{gap} and the increasing charge transfer among the donor, π -bridge, and the acceptor.

Acknowledgements

We are very grateful to Dr. Shian Zhang from the Key Laboratory of Optical and Magnetic Resonance Spectroscopy in East China Normal University, for the DFWM experiment and the helpful discussion. This research was financially supported by the National Natural Science Fund of China (Grant no. 20876148).

References

- [1] de la Torre G, Vaquez P, Agullo-Lopez F, Torres T. Role of structural factors in the nonlinear optical properties of phthalocyanines and related compounds. *Chem Rev.* 2004;104(9):3723-50.
- [2] Delaire JA, Nakatani K. Linear and nonlinear optical properties of photochromic molecules and materials. *Chem Rev.* 2000;100(5):1817-45.
- [3] Alicante R, Cases R, Forcen P, Oriol L, Villacampa B. Synthesis and Nonlinear Optical Properties of Side Chain Liquid Crystalline Polymers Containing Azobenzene Push-Pull Chromophores. *J Polym Sci Pol Chem.* 2010;48(1):232-42.
- [4] Zhu J, Huang X, Li JJ, Zhao JW. Theoretical calculation of enhancement factor of third-order nonlinear susceptibility in gold nanowire and nanotube. *J Optoelectron Adv M.* 2009;11(1):56-61.
- [5] Qin CX, Wang XM, Wang JJ, Mao JY, Yang JY, Dai LX, et al. The synthesis and photo-physical properties of a hemicyanine dye. *Dyes Pigments.* 2009;82(3):329-35.
- [6] Getmanenko YA, Hales JM, Balu M, Fu J, Zojer E, Kwon O, et al. Characterisation of a dipolar chromophore with third-harmonic generation applications in the near-IR. *J Mater Chem.* 2012;22(10):4371-82.
- [7] Martinez-Perdiguero J, Zhang YQ, Walker C, Etxebarria J, Folcia CL, Ortega J, et al. Second harmonic generation in laterally azo-bridged H-shaped ferroelectric dimesogens. *J Mater Chem.* 2010;20(23):4905-9.
- [8] Meng QH, Yan WF, Yu MJ, Huang DY. A study of third-order nonlinear optical properties for anthraquinone derivatives. *Dyes Pigments.* 2003;56(2):145-9.
- [9] de la Torre G, Vazquez P, Agullo-Lopez F, Torres T. Phthalocyanines and related compounds: organic targets for nonlinear optical applications. *J Mater Chem.* 1998;8(8):1671-83.
- [10] Lin WX, Cui YJ, Gao JK, Yu JC, Liang T, Qian GD. Six-branched chromophores with isolation groups: synthesis and enhanced optical nonlinearity. *J Mater Chem.* 2012;22(18):9202-8.
- [11] Sarojini BK, Narayana B, Ashalatha BV, Indira J, Lobo KG. Synthesis, crystal growth and studies on non-linear optical property of new chalcones. *J Cryst Growth.* 2006;295(1):54-9.

- [12] Kowalski K, Zakrzewski J, Palusiak M, Domagala S. Aryl (ferrocenyl)-capped ethenylazaferrocenes: synthesis, structure and electrochemistry. *New J Chem*. 2006;30(6):901-7.
- [13] Sylla M, Giffard M, Boucher V, Illien B, Mercier N, Phu XN. Nonlinear optical properties of chiral thiolates. *Synthetic Met*. 1999;102(1-3):1548-9.
- [14] Tian YP, Lu ZL, You XZ, Luo BS, Chen LR. Structure and third-order optical property - Studies on metal bridged biferrocene complexes. *Acta Chim Sinica*. 1999;57(10):1068-74.
- [15] Tian YP, Zhang ML, Hu ZJ, Hu HM, Wu JY, Zhang XJ, et al. Synthesis, crystal structure and NLO properties of a novel ruthenium(II) complex with unusual coordination mode. *Transit Metal Chem*. 2005;30(7):778-85.
- [16] Karabulut I, Baskoutas S. Linear and nonlinear optical absorption coefficients and refractive index changes in spherical quantum dots: Effects of impurities, electric field, size, and optical intensity. *J Appl Phys*. 2008;103(7).
- [17] Yang HY, Li LK, Song YL, Hou HW, Fan YT. Syntheses and characterization of ferrocenylthiocarboxylate-containing coordination compounds for nonlinear optics. *J Organomet Chem*. 2008;693(15):2624-30.
- [18] Andersson AS, Kerndrup L, Madsen AO, Kilsa K, Nielsen MB, La Porta PR, et al. Synthesis and characterization of tetrathiafulvalene-substituted di- and tetraethynylethenes with p-nitrophenyl acceptors. *J Org Chem*. 2009;74(1):375-82.
- [19] Robinson KL, Lawrence NS. Vinylferrocene homopolymer and copolymers: An electrochemical comparison. *Anal Sci*. 2008;24(3):339-43.
- [20] Calabrese JC, Cheng LT, Green JC, Marder SR, Tam W. Molecular 2nd-order optical nonlinearities of metallocenes. *J Am Chem Soc*. 1991;113(19):7227-32.
- [21] Kondo T, Hoshi H, Honda K, Einaga Y, Fujishima A, Kawai T. Photochemical modification of a boron-doped diamond electrode surface with vinylferrocene. *Journal of Physical Chemistry C*. 2008;112(31):11887-92.
- [22] Aloukos P, Iliopoulos K, Couris S, Guldi DM, Sooambar C, Mateo-Alonso A, et al. Photophysics and transient nonlinear optical response of donor- 60 fullerene hybrids. *J Mater Chem*. 2011;21(8):2524-34.
- [23] Barbero C, Calvo EJ, Etchenique R, Morales GM, Otero M. An EQCM electroacoustic study of poly(vinylferrocene) modified electrodes in different aqueous electrolytes. *Electrochim Acta*. 2000;45(22-23):3895-906.
- [24] Jureviciute I, Bruckenstein S, Hillman AR. Counter-ion specific effects on charge and solvent trapping in poly(vinylferrocene) films. *J Electroanal Chem*. 2000;488(1):73-81.
- [25] Xu CL, Chen JY, Aoki K. Partial charge transfer of poly(vinylferrocene)-coated latex particles adsorbed on pyrolytic graphite electrode. *Electrochem Commun*. 2003;5(6):506-10.
- [26] Issa TB, Singh P, Baker MV. Electrochemistry of poly(vinylferrocene) modified electrodes in aqueous acidic media. *J Power Sources*. 2005;140(2):388-91.
- [27] Gao JK, Cui YJ, Yu JC, Lin WX, Wang ZY, Qian GD. A 3-phenoxypropane-1, 2-diol based bichromophore for enhanced nonlinear optical properties. *Dyes Pigments*. 2010;87(3):204-8.
- [28] Lee C, Yang W, Parr RG. Development of the colle-Salvetti correlation-energy formula into a functional of the electron density. *Phys Rev B*. 1988;37(2):785-9.
- [29] Li W, Wu QF, Ye Y, Luo MD, Hu L, Gu YH, et al. Density functional theory and ab initio studies of geometry, electronic structure and vibrational spectra of novel benzothiazole and benzotriazole herbicides. *Spectrochim Acta A*. 2004;60(10):2343-54.

- [30] G. W. T. J. Frisch, H. B. Schlegel, G. E. Scuseria, M. A. Robb, J. R. Cheeseman, G. Scalmani, et al. Gaussian, Inc., Wallingford CT. 2009.
- [31] Pedulli GF, Todres ZV. High resolution EPR spectra of ferrocenyl(nitrophenyl)ethylene anion-radicals. *J Organomet Chem.* 1992;439(2):C46-C8.
- [32] Schlögl K, Egger H. Über Ferrocenderivate, XVIII. Synthese von Ferrocenyl-polyenen. *Justus Liebigs Annalen der Chemie.* 1964;676(1):76-87.
- [33] Sørensen T, Nielsen M. Synthesis, UV/vis spectra and electrochemical characterisation of arylthio and styryl substituted ferrocenes. *centeurjchem.* 2011;9(4):610-8.
- [34] Yasuda T, Abe J, Iyoda T, Kawai T. Selective Synthesis of 1-Aryl-2-ferrocenylethylene by Cross-Metathesis. *Chem Lett.* 2001;30(8):812-3.
- [35] Pang Y, Samoc M, Prasad PN. 3Rd-order nonlinearity and 2-photon-induced molecular-dynamics - femtosecond time-resolved transient absorption, kerr gate, and degenerate 4-wave-mixing studies in poly(para-phenylene vinylene) sol-gel silica film. *J Chem Phys.* 1991;94(8):5282-90.
- [36] Orczyk ME, Samoc M, Swiatkiewicz J, Prasad PN. Dynamics of 3rd-order nonlinearity of canthaxanthin carotenoid by the optically heterodyned phase-tuned femtosecond optical kerr gate. *J Chem Phys.* 1993;98(4):2524-33.
- [37] Cai ZB, Gao JR, Li XN. Synthesis and third-order optical nonlinearities of anthracenedione derivatives. *Dyes Pigments.* 2007;74(2):494-500.
- [38] Jenekhe SA, Chen WC, Lo SK, Flom SR. Large 3rd-order optical nonlinearities in organic polymer superlattices. *Appl Phys Lett.* 1990;57(2):126-8.
- [39] Ge Q, Corkery TC, Humphrey MG, Samoc M, Hor TSA. Organobimetallic Ru-II-Re-I 4-ethynylpyridyl complexes: structures and non-linear optical properties. *Dalton Transactions.* 2009(31):6192-200.
- [40] Ghosal S, Samoc M, Prasad PN, Tufariello JJ. Optical nonlinearities of organometallic structures - aryl and vinyl derivatives of ferrocene. *J PHYS CHEM.* 1990;94(7):2847-51.

Table 1. The values of $\chi^{(3)}$, γ , n_2 , and the respond times for 2a-2f.

sample	I	n	$\chi^{(3)}$ (10^{-13} esu)	n_2 (10^{-12} esu)	γ (10^{-31} esu)	Response time τ (fs)
2a	2.86776	1.4297	3.14	5.79	2.98	57.03
2b	1.90160	1.4294	2.55	4.01	2.42	51.34
2c	3.11582	1.4294	3.27	6.03	3.10	68.76
2d	4.18241	1.4286	3.78	6.98	3.60	51.67
2e	2.96993	1.4294	3.19	5.89	3.03	97.57
2f	3.06783	1.4295	3.24	5.98	3.08	55.46

Table 2. The energy (in eV) of the Highest Occupied Molecular Orbital (HOMO, E_{HOMO}), the Lowest Unoccupied Molecular Orbital (LUMO, E_{LUMO}), and the HOMO-LUMO gap (E_{gap}).

Compound	E_{HOMO}	E_{LUMO}	E_{gap}
2a	-5.111	-1.047	4.064
2b	-4.934	-0.844	4.090
2c	-5.394	-2.320	3.073
2d	-5.306	-1.447	3.860
2e	-4.973	-0.941	4.032
2f	-5.362	-2.146	3.215

Table 3. The Natural Charge (in e) of the complexes at the B3LYP/6-31G (d) level.

	2a	2b	2c	2d
π -bridge (-CH=CH-)	0.04	0.03	0.05	0.06
Substituents on aryl	-0.03	-0.01	-0.07	-0.07

Captions:

Fig.1 Synthetic routes of vinylferrocene derivatives.

Fig. 2 Optical path of DFWM.

Fig. 3 The UV-vis spectrum of 2a-2f in DMF.

Fig. 4 DFWM signal versus delay time for 2a-2f in DMF solution.

Fig. 5 The geometries optimized by B3LYP/6-31G (d) level.

Fig. 6 The energy of the highest occupied molecular orbital (HOMO) and the lowest unoccupied molecular orbital (LUMO) of the compound 2a to 2f.

Fig. 7 Frontier Molecular Orbitals of the compounds of 2a to 2f.

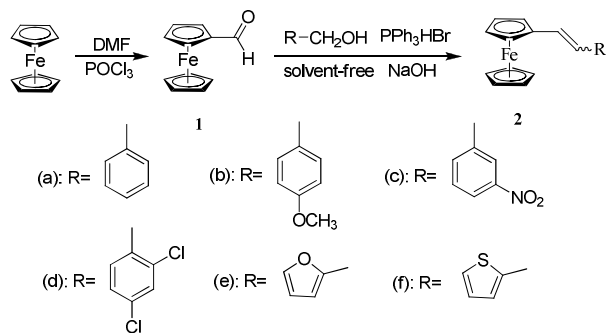


Fig.1 Synthetic routes of vinylferrocene derivatives.

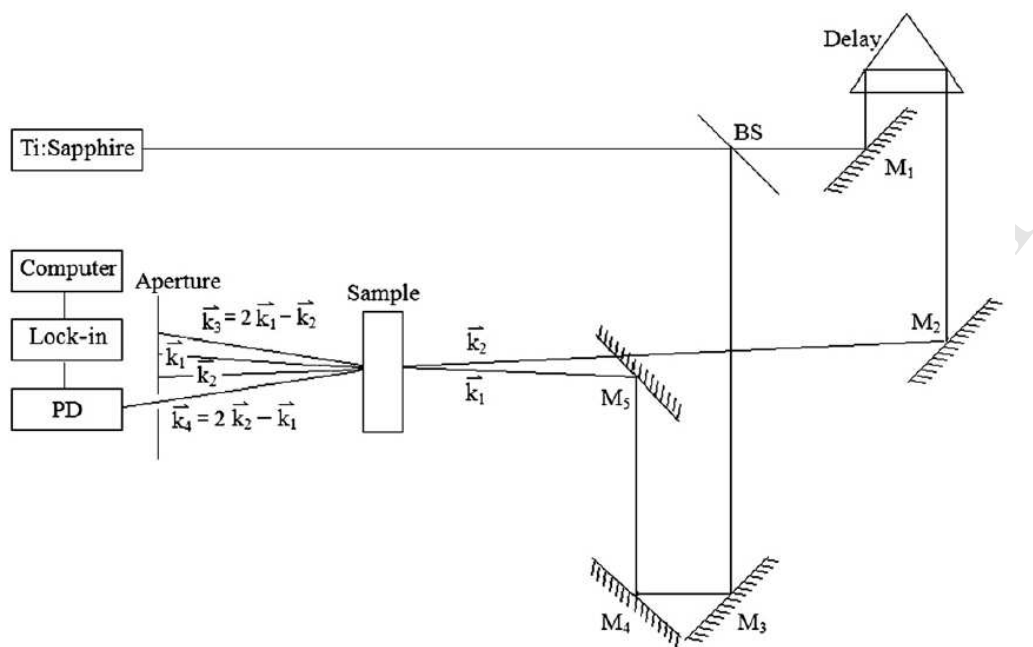


Fig. 2 Optical path of DFWM.

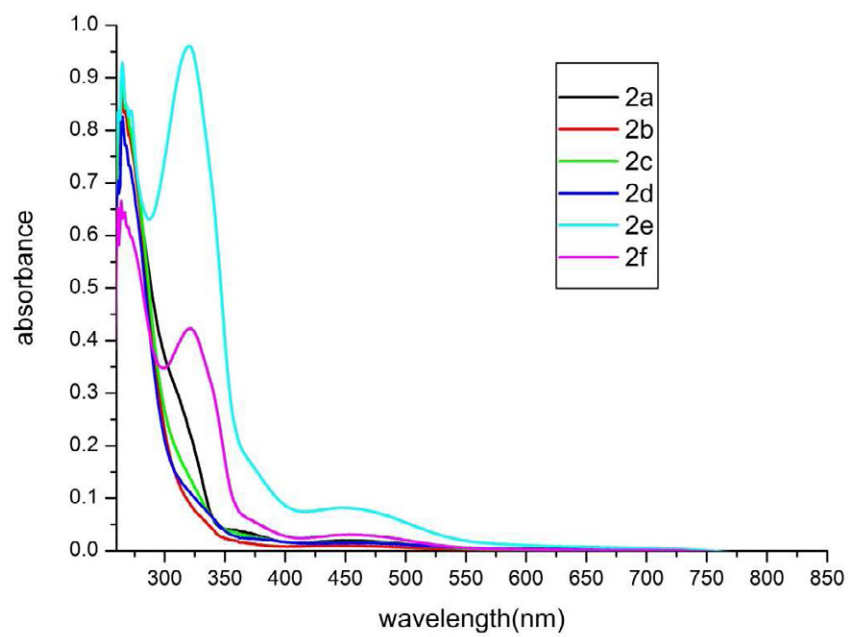


Fig. 3 The UV-vis spectrum of 2a-2f in DMF.

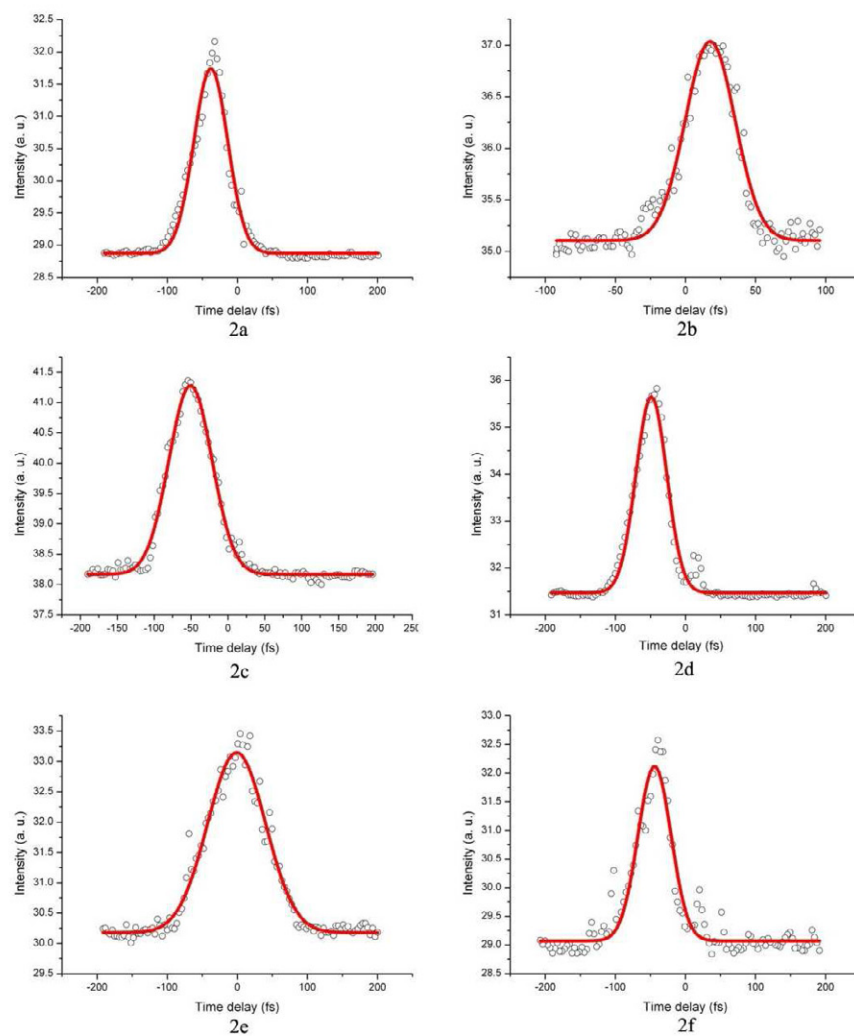


Fig. 4 DFWM signal versus delay time for 2a-2f in DMF solution.

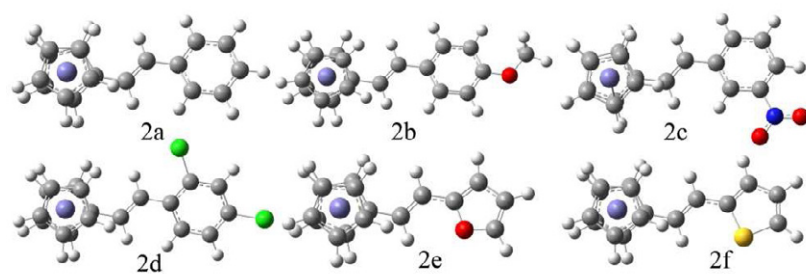


Fig. 5 The geometries optimized by B3LYP/6-31G (d) level.

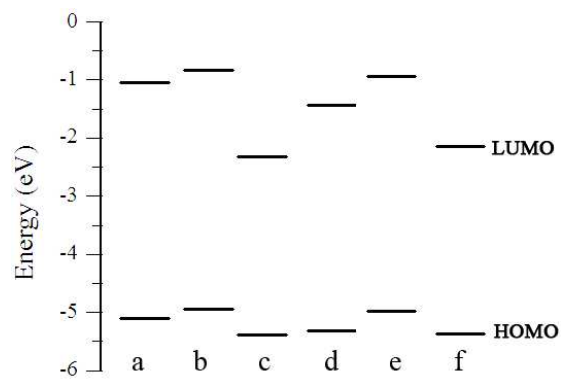


Fig. 6 The energy of the highest occupied molecular orbital (HOMO) and the lowest unoccupied molecular orbital (LUMO) of the compound 2a to 2f.

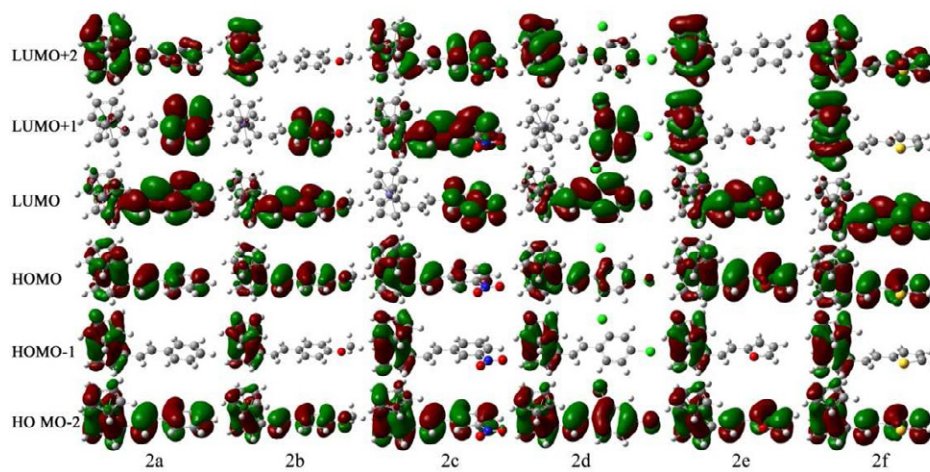


Fig. 7 Frontier Molecular Orbitals of the compounds of 2a to 2f.